Three-dimensional modeling of colloid and virus cotransport in porous media

Vasileios E. Katzourakis[1] and Constantinos V. Chrysikopoulos[2]

[1]Environmental Engineering Laboratory, Civil Engineering Department, University of Patras, Greece (billiskatz@yahoo.gr)

[2]School of Environmental Engineering, Technical University of Crete, Chania 73100, Greece (cvc@enveng.tuc.gr)

EGU2014-1406
Session HS8.1.7
Board Number R303

ΠΑΝΕΠΙΣΤΗΜΙΟ ΠΑΤΡΩΝ UNIVERSITY OF PATRAS

Technical University of Crete

BioNFate

Abstract

A conceptual mathematical model was developed to describe the simultaneous transport (cotransport) of viruses and colloids in three-dimensional, water saturated, homogeneous porous media with uniform flow. The model accounts for the migration of individual virus and colloid particles as well as viruses attached onto colloids. Viruses can be suspended in the aqueous phase, attached onto suspended colloids and the solid matrix, and attached onto colloids previously attached on the solid matrix. Colloids can be suspended in the aqueous phase or attached on the solid matrix. Viruses in all four phases (suspended in the aqueous phase, attached onto suspended colloid particles, attached onto the solid matrix, and attached onto colloids previously attached on the solid matrix) may undergo inactivation with different inactivation coefficients. The governing coupled partial differential equations were solved numerically by employing finite difference methods, which were implemented explicitly or implicitly so that both stability and accuracy factors were satisfied. Furthermore, pertinent experimental data published by Synguna and Chrysikopoulos (2013) were satisfactorily fitted by the newly developed cotransport model.

Model development

The colloid facilitated virus transport model assumes that the colloids partition between the aqueous phase and the solid matrix, while viruses attach onto colloid particles and the solid matrix. Consequently, colloid particles can be suspended in the aqueous phase, or attached onto the solid matrix. Viruses can be suspended in the aqueous phase, directly attached onto the solid matrix, attached onto suspended colloid particles (virus-colloid particles), and attached onto colloid particles that are already attached onto the solid matrix (or equivalently virus-colloid particles attached onto the solid matrix). A schematic illustration of the various types of concentrations considered in the present mathematical model is given in Fig. 1. To simplify the notation, the various masses are indicated as follows: M_c is the mass of colloids, M_v is the mass of viruses, and M_s is the mass of the solid matrix.

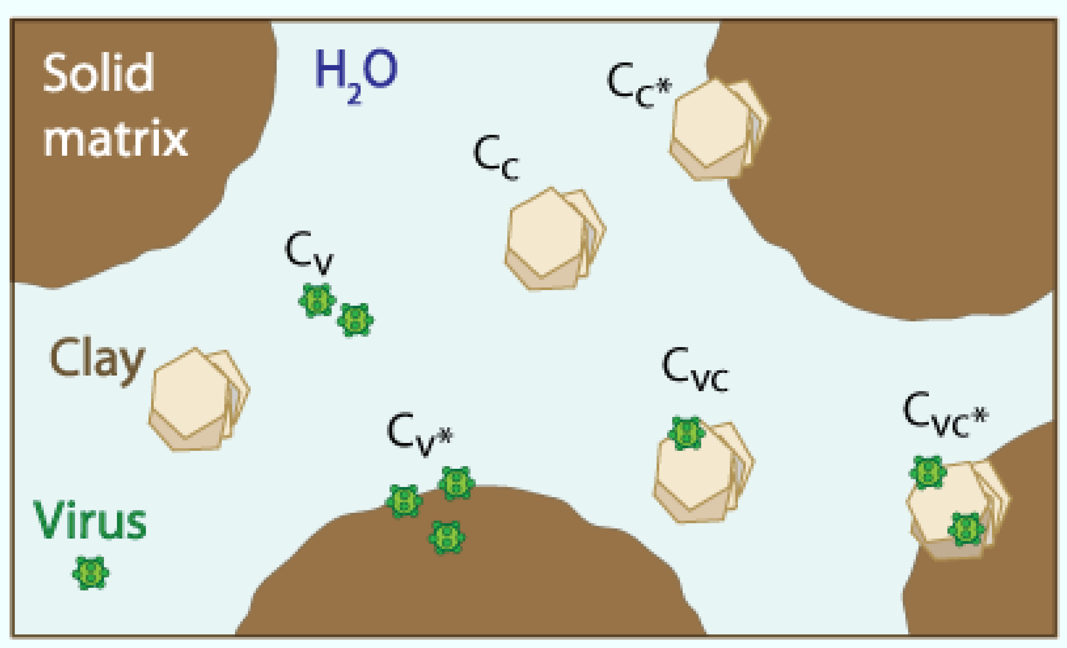

Figure 1: Schematic illustration of the various concentrations accounted for in the cotransport mathematical model.

- C_c colloid particles suspended in the aqueous phase $[M_c/L^3]$
- C_c^* colloid particles attached onto the solid matrix :
  - a) Due to adsorption $C_c^{*(r)}$ $[M_c/M_s]$ (r=reversible)
  - b) Due to deposition $C_c^{*(i)}$ $[M_c/M_s]$ (i= irreversible)
- C_v Viruses suspended in the aqueous phase $[M_v/L^3]$
- C_v^* Viruses Directly attached onto the solid matrix $[M_v/M_s]$
- C_{vc} Viruses attached onto suspended colloid particles (virus-colloid particles) $[M_v/M_c]$
- C_{vc}^* Viruses attached onto colloid particles that are already attached onto the solid matrix (or equivalently virus-colloid particles attached onto the solid matrix) $[M_v/M_c]$

Mathematical model

Governing partial differential equations

3-D Colloid transport equation

(Sim and Chrysikopoulos, 1998, 1999; Fabrice Compere et al., 2001)

$$\frac{\partial C_c(t,x,y,z)}{\partial t}+\frac{\rho_b}{\theta}\left[\frac{\partial C_c^{*(r)}(t,x,y,z)}{\partial t}+\frac{\partial C_c^{*(i)}(t,x,y,z)}{\partial t}\right]-D_{xc}\frac{\partial^2 C_c(t,x,y,z)}{\partial x^2}$$
$$-D_{yc}\frac{\partial^2 C_c(t,x,y,z)}{\partial y^2}-D_{zc}\frac{\partial^2 C_c(t,x,y,z)}{\partial z^2}+U\frac{\partial C_c(t,x,y,z)}{\partial x}=F_c$$

Colloid facilitated virus transport equation

(Vasiliadou and Chrysikopoulos, 2011)

$$\frac{\partial}{\partial t}\left(C_v+\frac{\rho_b}{\theta}C_v^*+C_cC_{vc}+\frac{\rho_b}{\theta}C_c^*C_{vc}^*\right)=D_{xv}\frac{\partial^2 C_v}{\partial x^2}+D_{xvc}\frac{\partial^2}{\partial x^2}(C_cC_{vc})+D_{yv}\frac{\partial^2 C_v}{\partial y^2}$$
$$+D_{yvc}\frac{\partial^2}{\partial y^2}(C_cC_{vc})+D_{zv}\frac{\partial^2 C_v}{\partial z^2}+D_{zvc}\frac{\partial^2}{\partial z^2}(C_cC_{vc})-U\frac{\partial}{\partial x}(C_v+C_cC_{vc})-\lambda_vC_v$$
$$-\lambda_{vc}C_vC_{vc}-\lambda_v^*\frac{\rho_b}{\theta}C_v^*-\lambda_{vc}^*\frac{\rho_b}{\theta}C_c^*C_{vc}^*+F_v$$

Suspended colloid-virus complex mass accumulation rate

(Bekhit et al., 2009)

$$\frac{\rho_b}{\theta}\frac{d}{dt}(C_c^*C_{vc}^*)=\frac{\rho_b}{\theta}r_{v-v^*c^*}(C^*_{vc_{eq}}-C_{vc}^*)^2C_c^*-\frac{\rho_b}{\theta}r_{v^*c^*-v}(C_c^*C_{vc}^*)+r_{vc-v^*c^*}(C_cC_{vc})$$
$$-\frac{\rho_b}{\theta}r_{v^*c^*-vc}(C_c^*C_{vc}^*)-\lambda_{vc}^*\frac{\rho_b}{\theta}C_c^*C_{vc}^*$$

Adsorbed colloid-virus complex mass accumulation rate

(Bekhit et al., 2009; Katzourakis and Chrysikopoulos, 2014)

$$\frac{d}{dt}(C_cC_{vc})=r_{v-vc}C_cC_v-r_{vc-v}(C_cC_{vc})+\frac{\rho_b}{\theta}r_{v^*c^*-vc}(C_c^*C_{vc}^*)$$
$$-r_{vc-v^*c^*}(C_cC_{vc})-\lambda_{vc}C_cC_{vc}$$

Reversible colloid adsorption 1st order equation

(Sim and Chrysikopoulos, 1998)

$$\frac{\rho_b}{\theta}\frac{\partial C_c^{*(r)}(t,x,y,z)}{\partial t}=r_{c\text{-}c^{*(r)}}C_c(t,x,y,z)-r_{c^{*(r)}\text{-}c}\frac{\rho_b}{\theta}C_c^{*(i)}(t,x,y,z)$$

Irreversible colloid adsorption 1st order equation

(Fabrice Compere et al., 2001)

$$\frac{\rho_b}{\theta}\frac{\partial C_c^{*(i)}(t,x,y,z)}{\partial t}=r_{c\text{-}c^{*(i)}}C_c(t,x,y,z)$$

Reversible virus adsorption 1st order equation

(Sim and Chrysikopoulos, 1998)

$$\frac{\rho_b}{\theta}\frac{\partial C_v^*(t,x,y,z)}{\partial t}=r_{v\text{-}v^*}C_v(t,x,y,z)-r_{v^*\text{-}v}\frac{\rho_b}{\theta}C_v^*(t,x,y,z)-\lambda_v^*\frac{\rho_b}{\theta}C_v^*(t,x,y,z)$$

The initial condition and the appropriate boundary conditions for the aquifer model employed in this study are as follows:

$$C_i(0,x,y,z)=0$$

$$-D\frac{\partial C_i(t,0,y,z)}{\partial x}+UC_i(t,0,y,z)=\begin{cases}UC_{0i}, & t\le t_p\\ 0, & t>t_p\end{cases}\qquad \frac{\partial C_i^2(t,L_x,y,z)}{\partial x^2}=0$$

$$\frac{\partial C_i(t,x,y,0)}{\partial z}=\frac{\partial C_i(t,0,y,L_z)}{\partial z}=0\qquad \frac{\partial C_i(t,x,0,z)}{\partial y}=\frac{\partial C_i(t,x,L_y,z)}{\partial y}=0$$

The fitting procedure

For the estimation of the unknown parameters, the commercial code Pest was used to fit the experimental data with the one-dimensional transport model. Pest is Model-Independent Parameter Estimation software and can adjust model parameters or excitation data so that the discrepancies between the pertinent model-generated numbers and the corresponding measurements are reduced to a minimum. For the needs of the fitting process some parameters were given from experiments in literature (status="Literature") while others had their values set, based on experimental data (status="Fixed").

Model application and simulations

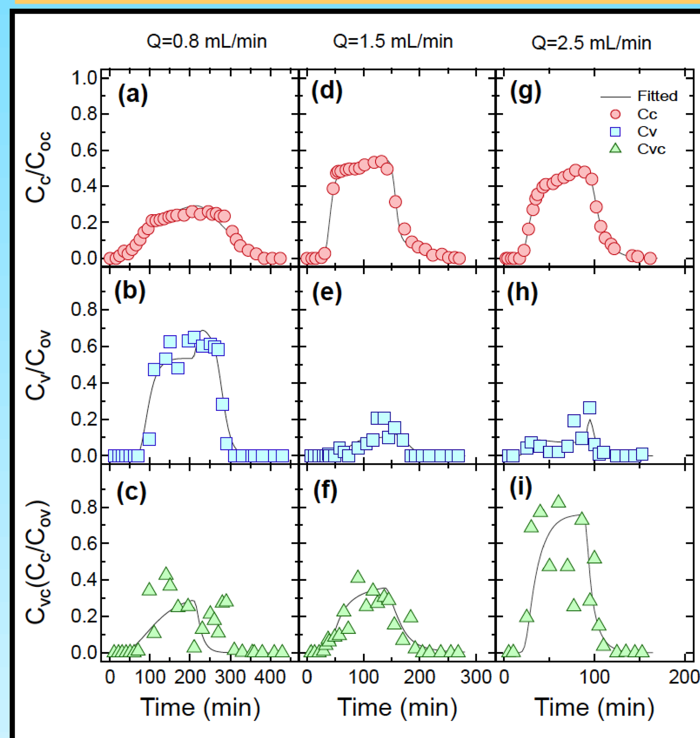

Figure 2: Breakthrough data of normalized (a,d,g) Cc, (b,e,h) Cv, and (c,f,i) Cvc from cotransport experiments with MS2 and KGa-1b conducted by Syngouna and Chrysikopoulos (2013) in columns packed with glass beads (symbols) and fitted model simulations (solid curves).

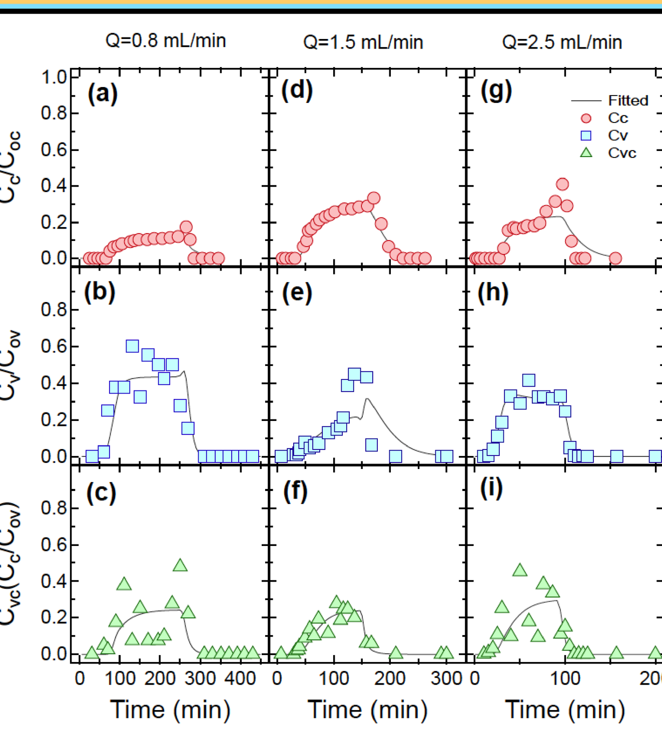

Figure 3: Breakthrough data of normalized (a,d,g) Cc, (b,e,h) Cv, and (c,f,i) Cvc from cotransport experiments with ΦX174 and KGa-1b conducted by Syngouna and Chrysikopoulos (2013) in columns packed with glass beads (symbols) and fitted model simulations (solid curves).

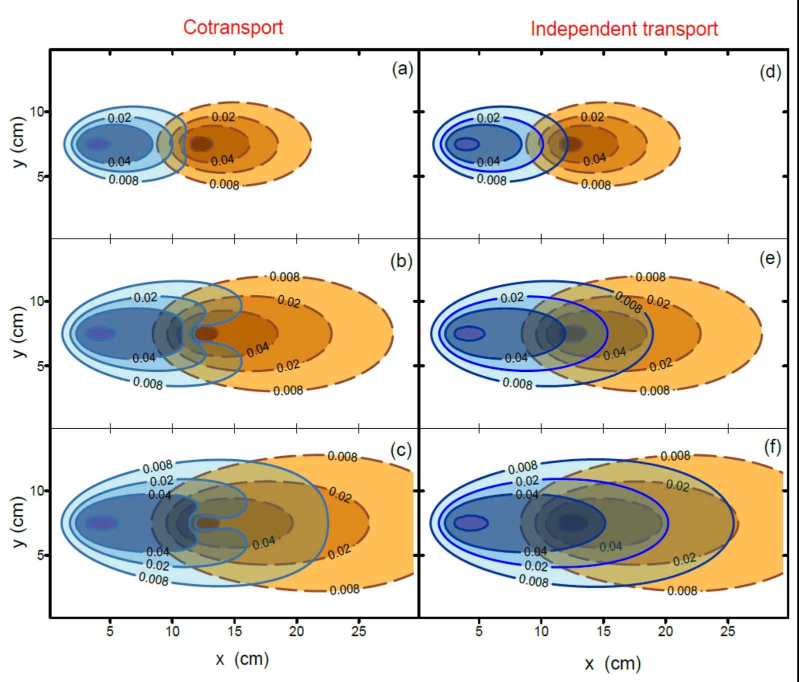

Figure 6: Contour plots on the x-y plane of virus (solid curves) and colloid (dashed curves) normalized concentrations, for the case of (a,b,c) cotransport, and (d,e,f) independent transport in a three-dimensional porous (L_X=30 cm, L_Y=15 cm, L_Z=10 cm) medium at three different times (t= 8 min, t=20 min and t=34 min), at z=5 cm.

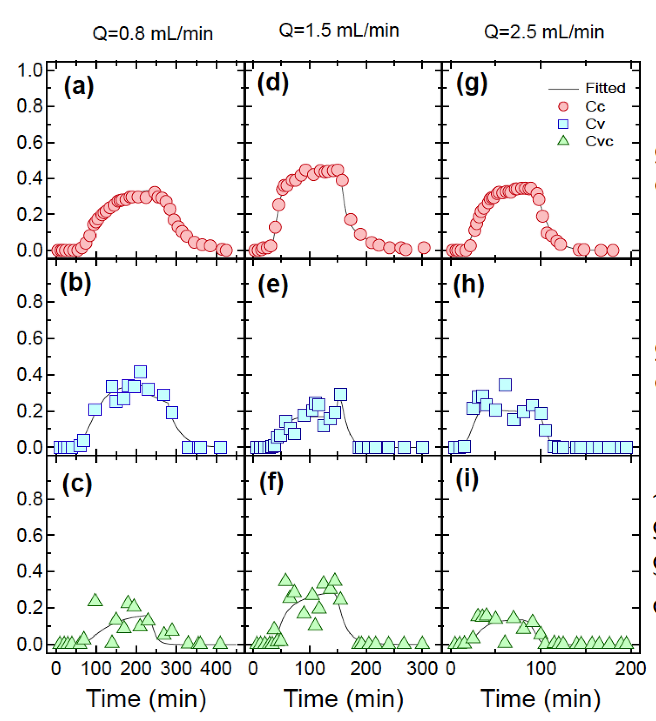

Figure 4: Breakthrough data of normalized (a,d,g) Cc, (b,e,h) Cv, and (c,f,i) Cvc from cotransport experiments with MS2 and STx-1b conducted by Syngouna and Chrysikopoulos (2013) in columns packed with glass beads (symbols) and fitted model simulations (solid curves).

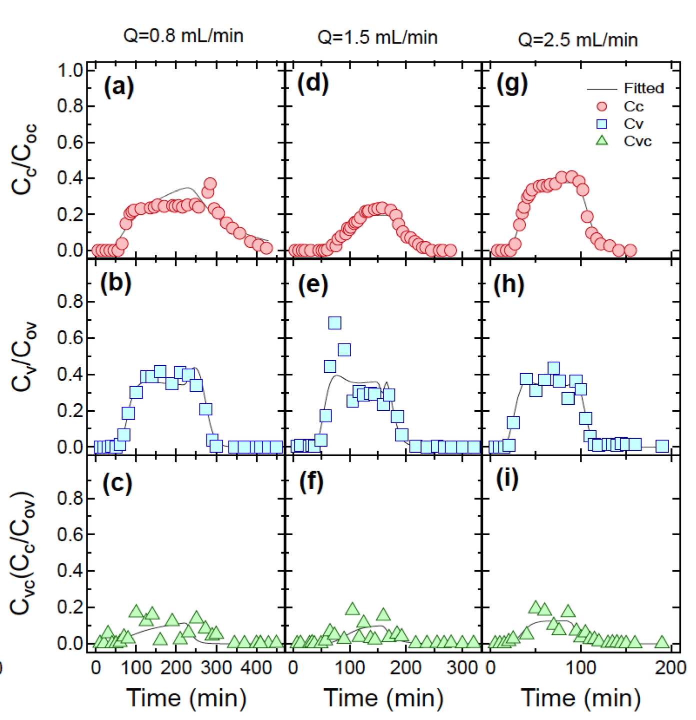

Figure 5: Breakthrough data of normalized (a,d,g) Cc, (b,e,h) Cv, and (c,f,i) Cvc from cotransport experiments with ΦX174 and STx-1b conducted by Syngouna and Chrysikopoulos (2013) in packed with glass beads (symbols) and fitted model simulations (solid curves).

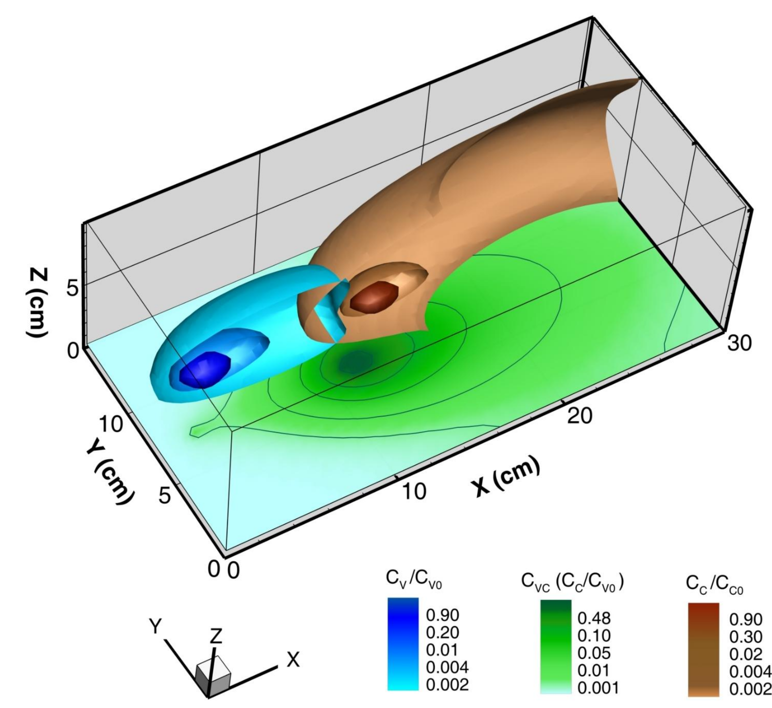

Figure 7: Isosurface three-dimensional plots of virus (blue surfaces) and colloid (brown surfaces) normalized concentrations, along with a projected x-y plane slice at z=5 cm, of the virus-colloid particles (green contour), at t=20 min.

Results

The experimental data from colloid-facilitated virus transport experiments in packed columns, conducted by Syngouna and Chrysikopoulos (2013), were fitted by the newly developed model. MS2 (exp. 1-3) and ΦX174 (exp. 4-6) were used as model viruses, and kaolinite (kGa-1b) as model clay colloids. Supplemental fittings were also carried based on montmorillonite (STx-1b). Interstitial velocity was set to 0.38 (exp. 1 and 4), 0.74 (exp. 2 and 5), and 1.21 (exp. 3 and 6) cm/min. Finally all cotransport experiments were conducted using a 30 cm long glass column with 2.5 cm diameter, which was packed with 2 mm diameter glass beads and placed horizontally.

Table 1 MS2-KGa1b (Exp. 1-3) and ΦX174-KGa-1b (Exp. 4-6) Fitted parameters

Parameter	Status	Exp. 1	Exp. 2	Exp. 3	Exp. 4	Exp. 5	Exp. 6	Units
D_{xc}	Literature	0.3	0.7	1.0	0.3	0.7	1.0	cm^2/min
D_{xv}	Literature	0.11	0.13	0.17	0.12	0.53	0.5	cm^2/min
D_{xvc}	Fixed	0.3	0.7	1.0	0.3	0.7	1.0	cm^2/min
U	Fixed	0.380	0.740	1.210	0.380	0.740	1.210	cm/min
$r_{v\text{-}vc}$	Fitted	0.002±0.001	0.015±0.01	0.063±0.01	0.009±0.02	0.34±0.08	0.08±0.06	cm^3/mg min
$r_{c\text{-}c^{*(i)}}$	Fitted	0.014±0.01	0.014±0.001	0.03±0.02	0.007±0.002	0.028±0.002	0.058±0.02	1/min
$r_{c\text{-}c^{*(r)}}$	Literature	0.037	0.006	0.045	0.01	0.078	0.081	1/min
$r_{c^{*(r)}\text{-}c}$	Fitted	0.12±0.05	0.021±0.01	0.138±0.05	0.042±0.002	0.112±0.01	0.12±0.01	1/min
ρ	Fixed	1610	1610	1610	1610	1610	1610	mg/cm^3

Notation

- F_i general form of species i source configuration, $[M_i/L^3t]$
- D_{ij} hydrodynamic dispersion coefficient of species i, at the j direction $[L^2/t]$
- λ_i decay rate of species i suspended in the liquid phase [1/t]
- L_i Length of the i dimension of the aquifer medium [L]
- $r_{i\text{-}i^*}$ attachment rate of species i onto the solid matrix [1/t]
- λ_i^* decay rate of species i attached onto the solid matrix [1/t]

References

Vasiliadou, I.A., and C.V. Chrysikopoulos, Water Resources Research, 47, W02543, doi:10.1029/2010WR009560, 2011.

Sim, Y., Chrysikopoulos, C.V., Advances Water Resources, 22, 507-519, 1999.

Sim, Y., Chrysikopoulos, C.V, Transport in Porous Media, 30(1), 87-112, 1998.

Fabrice Compere, Gilles Porel, Frederick Delay, Journal of Contaminant Hydrology 49 (2001) 1-21

Bekhit, H.M., M.A. El-Kordy, A.E. Hassan, J. Contam. Hydrol., 108: 152–167, 2009.

Syngouna, V.I., and C.V. Chrysikopoulos, Physicochemical and Engineering Aspects, 416, 56–65, doi:10.1016/j.colsurfa.2012.10.018, 2013.

Katzourakis, V.E., and C.V. Chrysikopoulos, Advances in Water Resources, 68, 62-73, doi:10.1016/j.advwatres.2014.03.001, 2014.

Acknowledgment

This research has been co-financed by the European Union (European Social Fund-ESF) and Greek National Funds through the Operational program "Education and Lifelong Learning" under the action Aristeia I (Code No. 1185).

European Union European Social Fund

OPERATIONAL PROGRAMME EDUCATION AND LIFELONG LEARNING investing in knowledge society

MINISTRY OF EDUCATION & RELIGIOUS AFFAIRS MANAGING AUTHORITY

Co-financed by Greece and the European Union

NSRF 2007-2013 programme for development EUROPEAN SOCIAL FUND

University of Patras Environmental Engineering Laboratory UPeeL